

SOUND EVENT TRIAGE: DETECTING SOUND EVENTS CONSIDERING PRIORITY OF CLASSES

Noriyuki Tonami[†], Keisuke Imoto[◇]

[†]Ritsumeikan University, Japan, [◇]Doshisha University, Japan

ABSTRACT

We propose a new task for sound event detection (SED): sound event triage (SET). The goal of SET is to detect a high-priority event while allowing misdetections of low-priority events where the extent of priority is given for each event class. In conventional methods of SED for targeting a specific sound event class, only information on types of target sound can be treated. To flexibly control more wealth of information on the target event, the proposed SET exploits not only types of target sound but also the extent to which each target sound is detected with priority. To implement SET, we apply a method that allows the system input of the priority of sound events to be detected, which is based on the class-level loss-conditional training. Results of the experiment using the URBAN-SED dataset reveal that our SET scheme achieves reasonable detection performance in terms of frame-based and intersection-based F-scores. In particular, the proposed method of SET outperforms the conventional SED method by around 10 percentage points for some events.

Index Terms— Sound event triage, sound event detection, Loss-conditional training

1. INTRODUCTION

In our everyday life, humans utilize much information obtained from various environmental sounds [1]. The automatic analysis of environmental sounds will lead to the realization of many applications, e.g., anomalous sound detection systems [2], life-logging systems [3], systems for hard-of-hearing persons [4], systems for smart cars [5], and monitoring systems [6].

Sound event detection (SED) [7] is a major task in environmental sound analysis, which identifies sound event classes (e.g., “dog barking,” “car passing by,” and “people walking”) with those time stamps. In conventional SED, many methods using the hidden Markov model (HMM) [8, 9] and non-negative matrix factorization (NMF) [10, 11] have been proposed. Recently, numerous deep neural network (DNN)-based SED methods have been developed. In DNN-based SED, the convolutional neural network (CNN) [12], recurrent neural network (RNN) [13], and convolutional bidirectional gated recurrent unit (CNN-BiGRU) [14] have been applied. Moreover, some studies have shown that the self-attention-based Transformer [15, 16] and Conformer [17] are useful for SED.

The target sounds to be analyzed depend on the user or application. In speech processing, source separation based on beamforming [18] for extracting a target speech from mixed sounds has been proposed. In music processing, to extract the sound intended by a user, a music separation method using the user’s humming [19] has been proposed. In the analysis of environmental sounds, universal sound selection [20], environmental sound extraction [21], and sound event localization and detection (SELD) [22] have been proposed. Okamoto *et al.* [21] have proposed a method of extracting

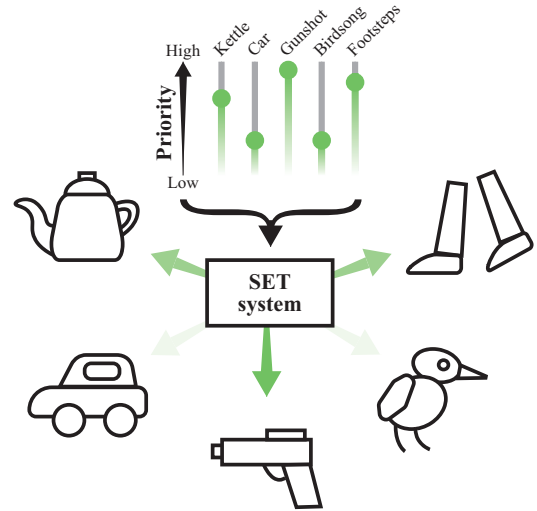


Fig. 1. Concept of SET

environmental sounds using onomatopoeia words intended by a user.

For SED, target sound detection (TSD) has been proposed by Yang *et al.* [23], in which only the target sound is detected, where a reference audio signal or a one-hot vector of the target sound is input to the TSD model. In SED, the goal is to generalize the performance of detecting all sound events, i.e., the SED models are trained to equally detect all sound events. In real environments, however, the detection priority for each event depends on the user or application. For example, when SED is used for a surveillance system, anomalous events such as “gunshot” or “baby crying” have to be preferentially detected over other events. On the other hand, in the case of a life-logging system, a sound event “kettle” or “footsteps” has to be more preferentially detected in addition to other events. In the conventional method for TSD, target events can be selected but the degree to which priority for detecting the target events cannot be controlled.

To tackle this problem, we propose a new SED task: **sound event triage (SET)**. The goal of SET is to improve the performance of detecting a high-priority sound event while allowing the performance of detecting a low-priority event to be compromised where the extent of priority is given for each event class; that is, the triage. In Fig. 1, the concept of SET is illustrated. SET enables user-preference sound event detection. The difference between the conventional methods for SED including TSD [23] and SET is whether the degree to which events are detected with priority can be set. We then propose a method for SET, in which a loss-conditional training [24] is utilized for detecting sound events with priority.

2. RELATED WORKS

In this section, we describe works related to the proposed method. In particular, the section comprises three subsections: strongly supervised SED, the conventional methods of environmental sound analysis using class-conditional techniques, and a loss-conditional method based on You Only Train Once (YOTO) [24], with which the arbitrary linear combination of loss weights for multiple tasks can be set with a single model.

2.1. Strongly supervised SED

In strongly supervised SED, given a SED model f , model parameters Θ , an acoustic feature \mathbf{X} , and a ground truth $z_{n,t} \in \{0, 1\}$ for a sound event n in time t , the SED model outputs the probability $y_{n,t}$ for the event n and time frame t :

$$y_{n,t} = P(z_{n,t} | f, \Theta, \mathbf{X}). \quad (1)$$

In the training of the DNN-based SED model, to optimize the model parameters Θ , the following binary cross-entropy (BCE) loss function is used:

$$\mathcal{L}_{\text{SED}} = - \sum_{n=1}^N \left\{ \mathbf{z}_n \log \sigma(\mathbf{y}_n) + (1 - \mathbf{z}_n) \log (1 - \sigma(\mathbf{y}_n)) \right\} \quad (2)$$

$$= - \sum_{n=1}^N \sum_{t=1}^T \left\{ z_{n,t} \log \sigma(y_{n,t}) + (1 - z_{n,t}) \log (1 - \sigma(y_{n,t})) \right\}, \quad (3)$$

where $\sigma(\cdot)$ denotes the sigmoid function. N and T are the numbers of sound event classes and total time frames, respectively. In an inference stage of SED, $\sigma(y_{n,t})$ is binarized with a predefined threshold to obtain detection results. As can be seen in Eq. 3, all sound events are equally weighted for generalizing the performance of detecting all sound events.

2.2. Methods of environmental sound analysis for targeting a specific sound

In the analysis of environmental sounds, several methods considering user-guided or target-class-conditioned information have been proposed [20, 21, 22, 23]. In the methods in [20, 21], environmental sound extraction systems utilize use-guided information. Ochiai *et al.* [20] have proposed a method that conditions the universal sound separation system with a multi-hot vector of target classes for extracting target event classes from a mixture of sound events. The system requires many pairs of an acoustic signal and a sound event label in a supervised manner. In works related to SED, TSD [23] and class-conditioned SELD where information on target event classes or sounds is employed [22] have been studied. Yang *et al.* [23] have proposed the TSD task derived from SED, which detects target sound events with a one-hot vector of the target event class. In the TSD network, a reference signal or a one-hot vector of the target event class is input to a network of the condition, which is embedded and then fused with a SED network. Slizovskaia *et al.* [22] have proposed the class-conditioned SELD, which analyzes a

specific-target event similarly to TSD to detect the target sound using a one-hot vector of the target class. These conventional systems related to SED can only handle information about the types of sound to be analyzed.

2.3. YOTO

YOTO [24] is a technique that enables a single network to perform various models, where each model has a different type of expertise, in inference stages. In the task of image compression, there is expertise for image quality and compression rate [24]. In this case, a single network using YOTO can perform various image-quality or compression-rate specialists in inference stages. The YOTO scheme is efficient in terms of the training cost or model complexity compared with multiple networks for each type of expertise.

In YOTO, we assume a problem setting that a single DNN-based network performs multiple tasks where the network is trained with multiple losses for each task. Let \mathcal{L}_m be a loss function for task m . The following loss function is often used for optimizing the parameters of the network:

$$\mathcal{L} = \sum_{m=1}^M \lambda_m \mathcal{L}_m, \quad (4)$$

where $\lambda_m (0 \leq \lambda_m \leq 1.0)$ is the weight of \mathcal{L}_m for balancing among the tasks. M denotes the number of tasks. In the training stage, the single network is trained with various λ_m values. In inference stages, an arbitrary λ_m can be input to the single network trained. When λ_m is set to be larger than those in other tasks, the network focuses on the training and/or inference of task m instead of other tasks.

3. PROPOSED METHOD

3.1. Framework of SET

In SET, not only types of target sound but also the degree of priority is used for conditioning models. In Fig. 2, the overview of SET in the training stage is shown. In the training stage of SET, triage weights are given for detecting target events with priority in addition to acoustic features and model parameters.

$$y_{n,t} = P(z_{n,t} | f, \mathbf{X}, \boldsymbol{\lambda}, \Theta), \quad (5)$$

where $\boldsymbol{\lambda} = (\lambda_1, \lambda_2, \dots, \lambda_N)$ are the parameters for the triage, that is, detecting sound events with priority. $\lambda_n (0 \leq \lambda_n \leq 1.0)$ is a triage weight for the sound event n . In an inference stage of SET, an arbitrary triage parameter $\boldsymbol{\lambda}$ is input to the SET model. When λ_n is set to a larger value than the others, the model targets with higher priority the sound event n than the other events. The loss functions on the right side in Fig. 2 are described in section 3.3.

3.2. Class-level loss-conditional training

In the DNN-based SED, as shown in Eq. 3, the BCE loss can be divided into losses of each event class. In other words, the BCE loss can be regarded as the sum of losses for the task of detecting each sound event class. To perform the event-class-level loss-conditional training of SET, the following loss function is used:

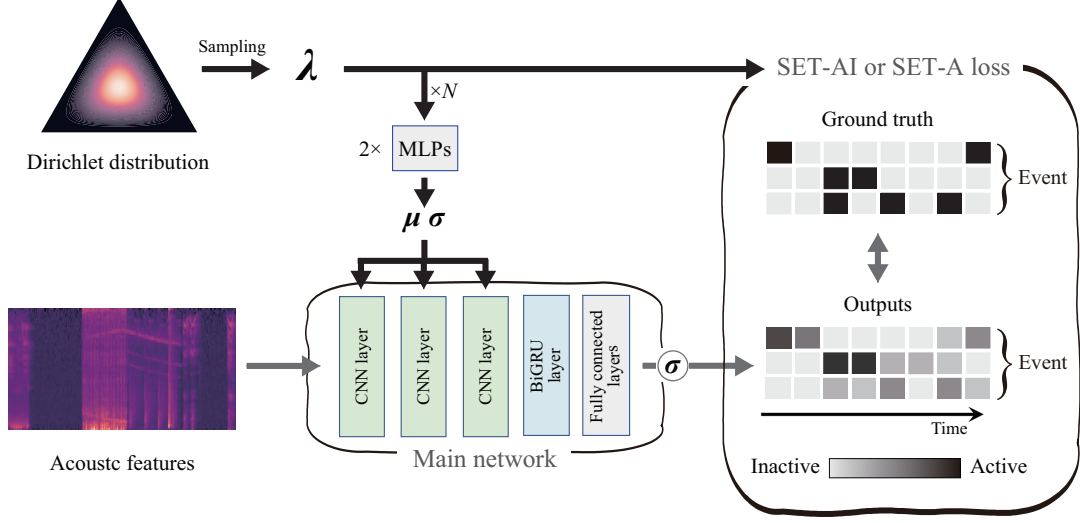


Fig. 2. Overview of SET in training stage

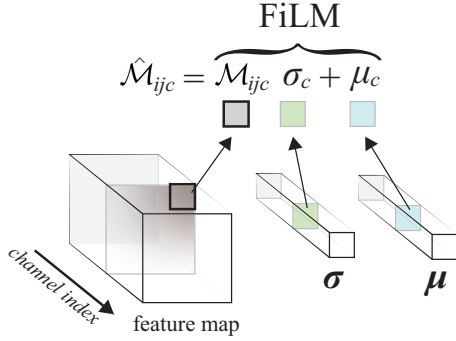


Fig. 3. Illustration of FiLM operation

$$\mathcal{L}_{\text{SET}} = \sum_{n=1}^N N \lambda_n \mathcal{L}_{\text{SED}}(n), \quad (6)$$

where λ_n and $\mathcal{L}_{\text{SED}}(n)$ indicate a triage weight and a loss function for sound event n , respectively. In Eq. 6, note that N is multiplied for scaling the loss function due to $\sum_n \lambda_n = 1.0$.

To use arbitrary λ_n in inference stages of a SET network, $\lambda = (\lambda_1, \lambda_2, \dots, \lambda_N)$ are repeatedly and randomly sampled from a distribution during the training, which cover various λ values in the single SET network. The sampled parameters λ are input to the SET network and used for the loss calculation (Eq. 6) in the training stage. As shown in Fig. 2, λ values are firstly fed to two multilayer perceptrons (MLPs). The MLPs output two vectors, $\mu = (\mu_1, \mu_2, \dots, \mu_C)$ and $\sigma = (\sigma_1, \sigma_2, \dots, \sigma_C)$. As shown in Fig. 3, feature-wise linear modulation (FiLM) [25] is then used to bridge between the outputs of the MLPs and the main network for detecting events (Fig. 2). The FiLM is applied to a feature map in CNN layers of the main network. The feature map is multiplied by σ and added to μ : $\hat{\mathcal{M}}_{ijk} = \mathcal{M}_{ijk} \sigma_c + \mu_c$. Here, \mathcal{M}_{ijk} is a feature at a location (i, j) of a channel index c in a feature map of a CNN layer, as shown in Fig. 3. In addition to the conditioning of the main network, the sampled

λ values are directly used for the losses (Eq. 6) in training stages.

As the distribution of the triage weight λ_n , we use the Dirichlet distribution $\mathcal{D}(\alpha)$. The probability density function of the $(K - 1)$ -dimensional Dirichlet distribution is

$$\mathcal{D}(\alpha) = \frac{\Gamma(\sum_{k=1}^K \alpha_k)}{\prod_{k=1}^K \Gamma(\alpha_k)} \prod_{k=1}^K x_k^{\alpha_k - 1}, \quad (7)$$

$$s.t. \sum_{k=1}^K x_k = 1, \quad (8)$$

where $x_k \geq 0$ and $\alpha_k > 0$ are stochastic variables for a dimension k and a parameter for the shape of the distribution. $\Gamma(\cdot)$ represent the gamma function. When α is small, the Dirichlet distribution is sharpened; that is, its shape is beneficial exclusively for the triage. Our SET is conditioned by the event-class-level YOTO, where the triage weight λ is sampled for each sound event class, to handle arbitrary λ , i.e., the extent of priority of the detection. N is also multiplied by inputs of the MLPs for conditioning the main network, as shown in Fig. 2.

3.3. SET losses with priority of event classes

To perform our SET, Eq. 6 is specified in this section. We propose two loss functions for the class-level loss-conditional training of SET. First, we introduce a loss function of SET with active and inactive frames (SET-AI) as follows.

$$\mathcal{L}_{\text{SET-AI}} = - \sum_{n=1}^N N \lambda_n \left\{ \mathbf{z}_n \log \sigma(\mathbf{y}_n) + (1 - \mathbf{z}_n) \log (1 - \sigma(\mathbf{y}_n)) \right\} \quad (9)$$

$$= - \sum_{n=1}^N \sum_{t=1}^T N \lambda_n \left\{ z_{n,t} \log \sigma(y_{n,t}) + (1 - z_{n,t}) \log (1 - \sigma(y_{n,t})) \right\} \quad (10)$$

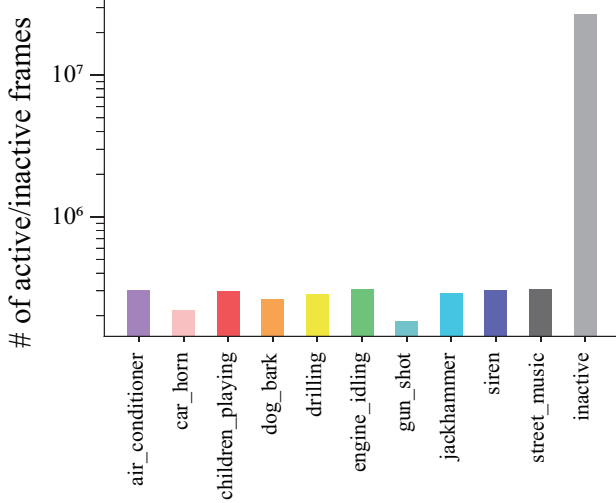


Fig. 4. Numbers of active and inactive frames for each event

In SET-AI, the triage weight λ_n affects the active and inactive frames of sound event n . When λ_n is set to a larger value than the others, the model focuses on the training and/or inference of the active and inactive frames of event n compared with the others. In SET-AI, the inactive frames are multiplied by λ_n .

A large number of inactive frames disturb the training of active frames, as reported in [26]. Hence, the number of only active frames is multiplied by λ_n . Thus, we also introduce a loss function of SET with active frames (SET-A), wherein the model focuses on the training of the active frames, as follows.

$$\mathcal{L}_{\text{SET-A}} = - \sum_{n=1}^N \left\{ N \lambda_n \mathbf{z}_n \log \sigma(\mathbf{y}_n) + (1 - \mathbf{z}_n) \log (1 - \sigma(\mathbf{y}_n)) \right\} \quad (11)$$

$$= - \sum_{n=1}^N \sum_{t=1}^T \left\{ N \lambda_n z_{n,t} \log \sigma(y_{n,t}) + (1 - z_{n,t}) \log (1 - \sigma(y_{n,t})) \right\} \quad (12)$$

The difference between SET-AI and SET-A is whether the number of inactive frames is multiplied by the triage weight λ_n .

4. EXPERIMENTS

4.1. Experimental conditions

To evaluate the effectiveness of our methods, we conducted the following experiments:

[Experiment 1]: We verified that the class-level loss-conditional training enables the detection of sound events with priority in terms of F-scores (sections 4.2.1 and 4.2.2).

[Experiment 2]: To analyze in more detail the properties of the proposed methods, we observed misdetection results in terms of insertion or deletion rate for the proposed methods (section 4.2.3).

Table 1. Experimental conditions

Main network	
Network architecture	3 CNN + 1 BiGRU + 2 FC
# channels of CNN layers	64, 64, 64
Filter size ($T \times F$)	3 × 3
Pooling size ($T \times F$)	8 × 1, 2 × 1, 2 × 1 (max pooling)
# of units in BiGRU layer	32
# of units in FC layers	128, 32
# of units in output layer	10
MLPs for each μ and σ	
Network architecture	3 FC
# of units in CNN layers	64, 256, 128
# of units in output layer	64
Optimizer	Adam [27]
Activation functions	leaky ReLU

For the experiments, we used the URBAN-SED [28] dataset. URBAN-SED includes 10,000 synthetic audio clips (train, 6,000; validation, 2,000; test, 2,000), where the duration of each clip is 10 s with a sampling rate of 44,100 Hz. The dataset consists of 10 sound event classes. In Fig. 4, the numbers of active and inactive frames for each event are indicated. As acoustic features, we used 64-dimensional log-mel band energies, which were calculated with the window size of 40 ms and the hop size of 20 ms. This setup is based on the baseline system of DCASE2018 Challenge task4 [29]. The threshold value of $\sigma(y_{n,t})$ was 0.5. The batch size was 64, and models were trained with 100 epochs. To measure the detection performance, we used frame-based and intersection-based metrics [30]. In the intersection-based metric, the detection tolerance criterion (DTC) and ground truth intersection criterion (GTC) are both set to 0.5.

As the main network in Fig. 2, we used two models. First, we used CNN-BiGRU [14], which is a combination of CNN and BiGRU. CNN-BiGRU is the widely used method as a baseline system for SED. Second, we used CNN-BiGRU with selective kernel units (CNN-BiGRU-SK) [31, 32], which achieved the best performance in DCASE2021 Challenge task4. In CNN-BiGRU-SK, kernels of multiple sizes are adopted in a CNN of a single model to handle various types of sound event. Other detailed parameters are shown in Table 1. In Table 1, “FC” means fully connected.

The FiLM operation ($\hat{m}_{ijc} = \sigma_c m_{ijc} + \mu_c$) was implemented between convolution and max pooling in each CNN layer. In this work, $\alpha_{\nu k}$ is set to 0.1 for the symmetric Dirichlet distribution $\mathcal{D}(\boldsymbol{\alpha})$, which was tuned using the train and validation set. K is set to the number of sound event classes.

4.2. Experimental results

4.2.1. [Experiment 1]: SET results in terms of frame-based F-score

In this experiment, we selected one target event class n for SET and then observed the F-scores of the target event class with various λ_n values in inference stages. The triage weight for a nontarget class is fixed at $1.0 / \sum_n \lambda_n$. For example, when the index of a target class is $n = 1$ and the triage weight λ_1 is set to $5.0 / \sum_n \lambda_n$, $\boldsymbol{\lambda} = (5.0, 1.0, \dots, 1.0) / \sum_n \lambda_n$. As aforementioned in section 3.2, N is multiplied by $\boldsymbol{\lambda}$ for the scaling before $\boldsymbol{\lambda}$ is input to the two MLPs for μ and σ .

Figure 5 shows the results of the proposed methods with various triage weights in terms of the frame-based F-score. In the legend, “Baseline” indicates the results obtained by the conventional methods CNN-BiGRU and CNN-BiGRU-SK using the BCE loss

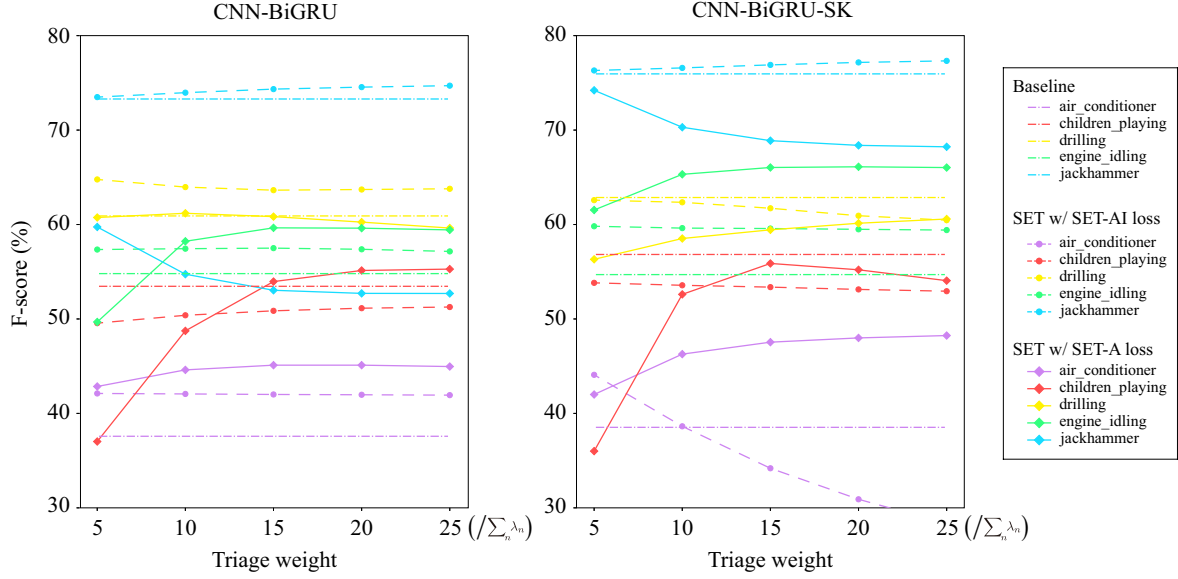


Fig. 5. SET results in terms of **frame-based** F-score for target classes with various triage weights

Table 2. SET results of **CNN-BiGRU** in terms of **frame-based** F-score (%) for target classes with various weights

Triage weight	Baseline	SET-AI loss					SET-A loss				
	-	5	10	15	20	25	5	10	15	20	25
air_conditioner	37.58	42.11	42.06	42.01	41.97	41.93	42.85	44.61	45.11	45.11	44.96
car_horn	59.50	56.36	56.76	56.92	57.00	57.04	57.22	58.40	59.06	58.90	58.87
children_playing	53.45	49.56	50.39	50.86	51.14	51.26	37.02	48.74	53.96	55.13	55.28
dog_bark	56.03	51.17	51.67	51.76	51.74	51.64	35.05	49.69	53.55	53.91	53.35
drilling	60.91	64.77	63.96	63.64	63.71	63.78	60.74	61.19	60.84	60.26	59.63
engine_idling	54.80	57.35	57.44	57.5	57.38	57.15	49.68	58.22	59.65	59.61	59.43
gun_shot	51.87	55.43	55.48	55.46	55.41	55.29	54.82	53.58	53.94	54.77	55.57
jack_hammer	73.29	73.49	73.96	74.34	74.55	74.70	59.74	54.74	53.04	52.71	52.70
siren	65.30	63.25	64.11	64.71	65.07	65.34	40.82	56.38	62.84	65.29	66.15
street_music	57.95	52.23	53.72	54.07	53.98	53.96	57.54	59.48	57.81	56.63	56.14

Table 3. SET results of **CNN-BiGRU-SK** in terms of **frame-based** F-score (%) for target classes with various weights

Triage weight	Baseline	SET-AI loss					SET-A loss				
	-	5	10	15	20	25	5	10	15	20	25
air_conditioner	38.52	44.09	38.64	34.19	30.91	28.32	42.00	46.28	47.54	47.99	48.24
car_horn	65.71	66.88	66.83	66.88	66.80	66.68	67.26	69.13	67.13	64.02	61.48
children_playing	56.83	53.82	53.57	53.37	53.13	52.94	36.01	52.60	55.88	55.21	54.06
dog_bark	57.81	57.23	56.86	56.66	56.38	56.14	49.03	59.27	59.22	57.48	55.65
drilling	62.86	62.58	62.35	61.72	60.93	60.46	56.32	58.52	59.44	60.14	60.58
engine_idling	54.70	59.82	59.62	59.57	59.49	59.41	61.54	65.31	66.04	66.11	66.03
gun_shot	56.25	58.98	58.42	57.25	56.51	56.09	59.77	63.54	61.97	60.73	59.54
jack_hammer	75.95	76.31	76.58	76.90	77.16	77.33	74.21	70.30	68.88	68.38	68.23
siren	66.14	67.95	67.88	67.45	67.06	66.79	62.48	59.51	57.78	56.67	55.86
street_music	57.90	61.82	61.17	60.50	60.05	59.68	52.31	63.17	61.85	60.42	59.52

Table 4. SET results of CNN-BiGRU in terms of intersection-based F-score (%) for target classes with various weights

Triage weight	Baseline	SET-AI loss					SET-A loss				
	-	5	10	15	20	25	5	10	15	20	25
air_conditioner	19.88	18.72	17.69	17.76	17.38	17.35	19.15	19.49	19.58	19.26	19.48
car_horn	47.41	47.39	47.28	46.43	45.94	46.02	41.20	38.72	37.23	35.99	35.58
children_playing	26.28	21.28	20.37	19.78	19.20	19.02	22.51	25.92	25.21	23.25	22.85
dog_bark	28.85	24.72	24.69	23.54	22.17	21.29	27.32	29.40	26.00	22.05	19.34
drilling	38.88	30.46	28.56	27.97	27.70	27.85	39.14	36.09	34.25	32.85	31.52
engine_idling	29.28	26.66	26.57	26.24	26.42	26.82	26.66	27.44	26.59	25.45	24.49
gun_shot	39.90	41.14	40.19	38.94	38.30	38.02	31.45	25.47	24.78	25.17	25.18
jack_hammer	44.51	42.68	43.74	44.14	44.60	44.45	29.12	26.26	25.02	24.14	23.67
siren	44.91	47.36	45.45	44.75	44.58	42.94	35.40	44.73	45.24	43.70	41.83
street_music	29.61	28.07	24.86	22.70	21.45	20.25	35.23	29.94	26.01	24.19	22.86

Table 5. SET results of CNN-BiGRU-SK in terms of intersection-based F-score (%) for target classes with various weights

Triage weight	Baseline	SET-AI loss					SET-A loss				
	-	5	10	15	20	25	5	10	15	20	25
air_conditioner	22.75	24.38	22.65	19.48	16.69	15.45	18.58	20.27	20.52	20.00	19.71
car_horn	54.51	53.89	53.23	52.01	50.82	50.02	61.95	56.82	47.11	41.15	37.56
children_playing	30.61	28.79	26.83	25.36	24.47	23.82	27.19	32.76	28.96	25.71	24.37
dog_bark	32.54	29.56	28.19	27.41	26.54	25.80	40.93	37.33	31.49	26.77	24.00
drilling	45.42	39.08	39.79	39.27	39.20	38.05	30.28	31.64	32.19	32.74	33.07
engine_idling	39.14	42.05	42.17	42.22	41.56	40.68	36.33	37.37	35.60	34.12	33.03
gun_shot	43.10	44.58	45.02	42.23	41.27	40.74	50.92	42.53	36.63	32.59	30.20
jack_hammer	48.83	48.28	46.97	46.36	46.55	46.68	44.76	38.78	36.91	35.85	34.94
siren	45.94	45.38	40.88	38.32	36.41	35.13	33.46	30.75	28.99	28.01	26.88
street_music	32.01	32.73	28.64	26.89	25.46	24.57	40.28	36.73	30.44	27.87	26.37

function. “SET-AI loss” and “SET-A loss” are SET with the class-level loss-conditional training using Eqs. 10 and 12, respectively. The results show that the proposed SET methods using the class-level loss-conditional training achieved a reasonable performance. The performance of detecting sound events “air_conditioner,” “children_playing,” and “engine_idling” gradually increases with the triage weight. Moreover, the performance of detecting those sound events markedly increases when using the SET-A loss compared with using the SET-AI loss. This is because the number of inactive frames of the sound events is large in the training set, as can be seen in Fig. 4. In other words, the models using the SET-AI loss might focus on the training of inactive frames. This leads to the degradation of the detection performance, as reported in [26]. On the other hand, the results of the sound events “drilling” and “jackhammer” indicate a different trend from those of “air_conditioner,” “children_playing,” and “engine_idling.” As the triage weight becomes larger, the detection performance using the SET-A loss is much more degraded than that using the SET-AI loss. This might be because “drilling” is acoustically similar to “jackhammer.” In [33], the timbre of these two events is similar and could also be confused in the classification task. The SET-A loss, which focuses on the active frames, may detect a target sound event and similar one simultaneously compared with the SET-AI loss.

Tables 2 and 3 show detailed SET results in terms of frame-based F-score for each target class with various weights based on CNN-BiGRU and CNN-BiGRU-SK, respectively. As shown in Table 2, many sound events are well detected using the pro-

posed methods compared with the baseline system. Notably, the detection performance of the proposed method using the SET-A loss is higher than that of the proposed method using the SET-AI loss. For events detected using the SET-A loss, the sound events “air_conditioner,” “children_playing,” “engine_idling,” “siren,” and “street_music” were detected better than when using the baseline system and the method using the SET-AI loss. In particular, the proposed method using the SET-A loss improved the frame-based F-score of “air_conditioner” by 7.53 and 9.72 percentage points compared with the conventional CNN-BiGRU and CNN-BiGRU-SK, respectively. Moreover, the proposed method using the SET-A loss of “street_music” achieved better performance in terms of the F-score than did the conventional CNN-BiGRU and CNN-BiGRU-SK. These well-detected events “air_conditioner” and “street_music” are characterized as continuous sounds, as reported in [34], which are relatively easy to detect than the others. The proposed method using SET-A mainly focuses on the active frames in Eq. 12, which would detect more active frames regardless of some misdetections and is good at detecting such continuous sounds with a number of active frames.

4.2.2. [Experiment 1]: SET results in terms of intersection-based F-score

We also evaluated the proposed methods in terms of the intersection-based F-score. In the intersection-based F-score, unlike the frame-based F-score, models are evaluated instance by instance. Here, “in-

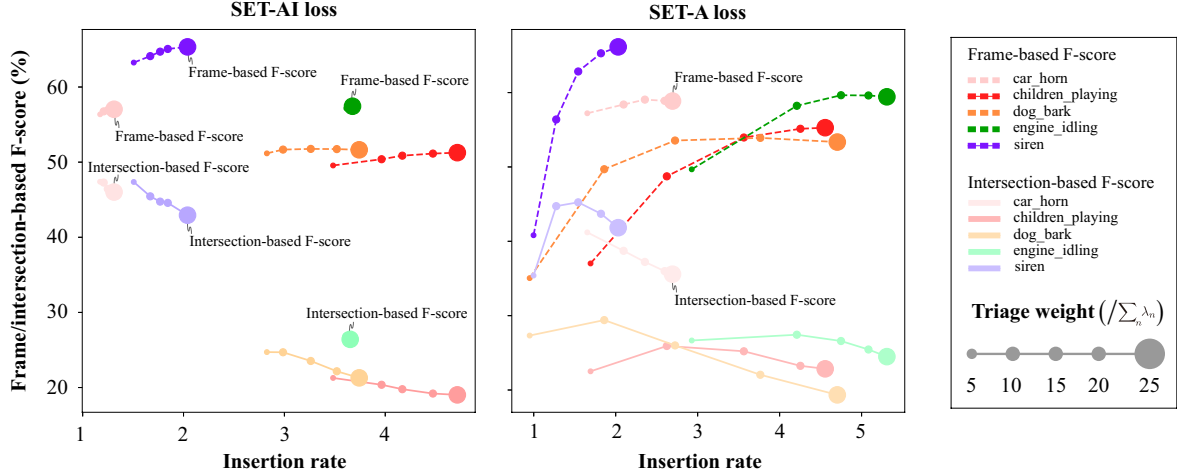


Fig. 6. Relationships between F-scores and insertion rate with various triage weights for CNN-BiGRU

Table 6. SET results of CNN-BiGRU in terms of IR for target classes with various weights

Triage weight	Baseline	SET-AI loss					SET-A loss				
	-	5	10	15	20	25	5	10	15	20	25
air_conditioner	1.83	3.13	3.41	3.51	3.62	3.67	4.10	3.83	3.75	3.72	3.67
car_horn	1.49	1.17	1.21	1.25	1.31	1.31	1.65	2.10	2.36	2.60	2.69
children_playing	2.98	3.48	3.96	4.17	4.47	4.71	1.69	2.62	3.56	4.25	4.56
dog_bark	2.79	2.83	2.99	3.26	3.52	3.74	0.95	1.86	2.72	3.76	4.70
drilling	1.93	3.91	4.37	4.54	4.61	4.58	2.24	2.81	3.23	3.49	3.75
engine_idling	2.51	3.64	3.68	3.66	3.65	3.61	2.93	4.21	4.75	5.08	5.31
gun_shot	1.46	1.59	1.67	1.72	1.78	1.85	2.81	3.93	4.33	4.35	4.38
jack_hammer	2.48	2.77	2.71	2.68	2.67	2.71	4.56	5.10	5.37	5.58	5.72
siren	1.60	1.51	1.67	1.77	1.84	2.04	1.00	1.27	1.54	1.82	2.03
street_music	3.12	2.83	3.52	4.20	4.74	5.08	2.21	3.69	4.65	5.12	5.50

Table 7. SET results of CNN-BiGRU in terms of DR for target classes with various weights

Triage weight	Baseline	SET-AI loss					SET-A loss				
	-	5	10	15	20	25	5	10	15	20	25
air_conditioner	0.88	0.84	0.84	0.84	0.84	0.84	0.77	0.79	0.80	0.81	0.82
car_horn	0.62	0.68	0.67	0.66	0.67	0.67	0.62	0.56	0.55	0.55	0.55
children_playing	0.83	0.87	0.86	0.85	0.85	0.85	0.93	0.87	0.83	0.80	0.79
dog_bark	0.82	0.87	0.86	0.85	0.85	0.85	0.94	0.87	0.85	0.83	0.84
drilling	0.69	0.60	0.59	0.59	0.59	0.59	0.65	0.63	0.63	0.61	0.60
engine_idling	0.80	0.79	0.78	0.79	0.80	0.81	0.84	0.76	0.73	0.72	0.71
gun_shot	0.83	0.82	0.83	0.82	0.82	0.82	0.74	0.73	0.74	0.74	0.73
jack_hammer	0.41	0.48	0.48	0.47	0.47	0.48	0.47	0.51	0.53	0.53	0.52
siren	0.70	0.74	0.73	0.73	0.73	0.73	0.89	0.80	0.76	0.73	0.70
street_music	0.77	0.84	0.84	0.84	0.85	0.85	0.78	0.68	0.70	0.70	0.72

stance” means a block with the associated onset and offset [35]. Tables 4 and 5 are SET results in terms of the intersection-based F-score compared with those of CNN-BiGRU and CNN-BiGRU-SK for various triage weights. The results show that the F-score of the proposed SET method is improved compared with that of the baseline system. In particular, as shown in Table 5, the proposed method

using the SET-A loss improved the intersection-based F-scores of the sound events “car_horn,” “dog_bark,” and “gun_shot” by 7.44, 8.39, and 7.82 percentage points compared with the conventional CNN-BiGRU-SK. As shown in Table 4, these events were not precisely detected using the proposed method. This implies that more sophisticated event detection methods can boost SET performance,

which needs to be investigated in future works. Unlike the results in terms of the frame-based F-score, the performance of detecting many sound events gradually deteriorates as the triage weight increases. This issue will be discussed in the next experiment.

4.2.3. [Experiment 2]: SET results of relationships among misdetections and F-scores

To investigate in more detail performance of SET, we used the error-related evaluation metrics, frame-based insertion rate (IR) and deletion rate (DR). Given false positives (FPs) and false negatives (FNs) for each event and time frame t , IR and DR are defined using the insertion (I) and deletion (D) [35] as follows:

$$I(t) = \max(0, FP(t) - FN(t)) \quad (13)$$

$$D(t) = \max(0, FN(t) - FP(t)) \quad (14)$$

$$IR = \sum_{t=1}^T \frac{I(t)}{A(t)}, \quad (15)$$

$$DR = \sum_{t=1}^T \frac{D(t)}{A(t)}, \quad (16)$$

where $FP(t)$ and $FN(t)$ are the numbers of FPs and FNs at frame t , respectively. $A(t)$ represents the number of active events at frame t .

The aforementioned results indicated the different behaviors between the frame-based and intersection-based F-scores. Figure 6 shows the relationships between the frame-base and intersection-based F-scores and insertion rate with various triage weights for each target event. In the figure, dashed lines indicate results of the relationships between the frame-based F-score and IR. Solid lines are results of the relationships between the intersection-based F-score and IR. The left figure shows that, by using the SET-AI loss, the intersection-based F-score for each target event is moderately decreased as the triage weight increases. As shown on the right side of Fig. 6, by using the SET-A loss, the frame-based F-score for each target event is highly increased as the triage weight increases. On the other hand, the result indicates that the intersection-based F-scores for most target events increase and then decrease as the triage weight increase. This is because the number of FPs is dominant in terms of the intersection-based F-score and is counted differently from that for the frame-based F-score, when the triage weight is set to be large. As shown in Fig. 7, the number of FPs is counted instance by instance in terms of the intersection-based F-score. Figure 7(a) shows an example of an instance for FPs. In Fig. 7(b), the detection result is divided into two instances, each of which is short. In the intersection-based F-score, the number of FPs in Fig. 7(b) is twice that in Fig. 7(a); that is, one instance is divided into multiple short instances with a significant impact. On the other hand, in the frame-based F-score, there is no large difference in the number of FPs between Figs. 7(a) and 7(b).

Tables 6 and 7 show results in terms of IR and DR for each target event with various triage weights. The results show that the IR of many events is worse than DR; that is, the systems are affected mainly by FPs. The proposed methods using the SET-A loss degrade IR compared with those using the SET-AI loss. This is because the SET-A loss focuses on recognizing active frames while it neglects inactive frames.

From the results in this section, we conclude that our SET detects more active frames for target events, but the number of divided or short-instance FPs might be increased.

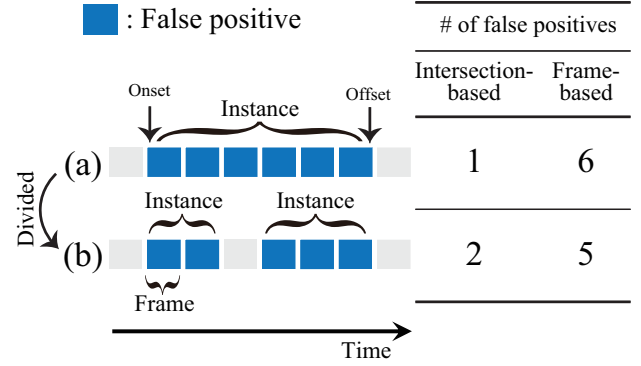


Fig. 7. How the number of FPs is counted for intersection- and frame-based F-scores

5. CONCLUSION

In this work, we proposed a new task for SED: sound event triage (SET), in which both the type of target sound and the extent of priority are considered for targeting specific sound events. To perform SET, the task-level conditional-loss training, where a model and loss are conditioned with sampled parameters, is utilized for detecting events with priority. Results of the experiments using the URBAN-SED dataset show that the proposed methods achieve reasonable detection performance in terms of the F-scores. The proposed method mainly considering active frames outperforms the conventional SED method by around 10 percentage points in terms of the frame-based F-score for some events. As the limitation of the proposed methods, the results indicate that the confusion errors among similar events might be enhanced.

6. REFERENCES

- [1] K. Imoto, "Introduction to acoustic event and scene analysis," *Acoustical Science and Technology*, vol. 39, no. 3, pp. 182–188, 2018.
- [2] Y. Koizumi, S. Saito, H. Uematsum, Y. Kawachi, and N. Harada, "Unsupervised detection of anomalous sound based on deep learning and the Neyman-Pearson lemma," *IEEE/ACM Trans. Audio, Speech, and Language Processing*, vol. 27, no. 1, pp. 212–224, 2019.
- [3] J. Stork, L. Spinello, J. Silva, and K. O. Arras, "Audio-based human activity recognition using non-Markovian ensemble voting," in *Proc. IEEE International Symposium on Robot and Human Interactive Communication (RO-MAN)*, 2012, pp. 509–514.
- [4] Y.-T. Peng, C.-Y. Lin, M.-T. Sun, and K.-C. Tsai, "Healthcare audio event classification using hidden Markov models and hierarchical hidden Markov models," in *Proc. IEEE International Conference on Multimedia and Expo (ICME)*, 2009, pp. 1218–1221.
- [5] M. Nandwana and T. Hasan, "Towards smart-cars that can listen: Abnormal acoustic event detection on the road," in *Proc. INTERSPEECH*, 2016, pp. 2968–2971.
- [6] S. Ntalampiras, I. Potamitis, and N. Fakotakis, "On acoustic surveillance of hazardous situations," in *Proc. IEEE International Conference on Acoustics, Speech and Signal Processing (ICASSP)*, 2009, pp. 165–168.

- [7] A. Mesaros, T. Heittola, T. Virtanen, and M. D. Plumbley, "Sound event detection: A tutorial," *IEEE Signal Processing Magazine*, vol. 38, no. 5, pp. 67–83, 2021.
- [8] A. Mesaros, T. Heittola, A. Eronen, and T. Virtanen, "Acoustic event detection in real life recordings," in *Proc. European Signal Processing Conference (EUSIPCO)*, 2010, pp. 1267–1271.
- [9] T. Heittola, A. Mesaros, A. Eronen, and T. Virtanen, "Context-dependent sound event detection," *EURASIP Journal on Audio, Speech, and Music Processing*, vol. 2013, no. 1, pp. 1–13, 2013.
- [10] J. Gemmeke, L. Vuegen, P. Karsmakers, B. Vanrumste, and H. Van hamme, "An exemplar-based NMF approach to audio event detection," in *Proc. IEEE Workshop on Applications of Signal Processing to Audio and Acoustics (WASPAA)*, 2013, pp. 1–4.
- [11] T. Komatsu, T. Toizumi, R. Kondo, and Y. Senda, "Acoustic event detection method using semi-supervised non-negative matrix factorization with mixtures of local dictionaries," in *Proc. Workshop on Detection and Classification of Acoustic Scenes and Events (DCASE)*, 2016, pp. 45–49.
- [12] S. Hershey, S. Chaudhuri, D. Ellis, J. Gemmeke, A. Jansen, C. Moore, M. Plakal, D. Platt, R. Saurous, B. Seybold, M. Slaney, R. Weiss, and K. Wilson, "CNN architectures for large-scale audio classification," in *Proc. IEEE International Conference on Acoustics, Speech and Signal Processing (ICASSP)*, 2017, pp. 131–135.
- [13] T. Hayashi, S. Watanabe, T. Toda, T. Hori, J. Le Roux, and K. Takeda, "Duration-controlled LSTM for polyphonic sound event detection," *IEEE/ACM Trans. Audio, Speech, and Language Processing*, vol. 25, no. 11, pp. 2059–2070, 2017.
- [14] E. Çakır, G. Parascandolo, T. Heittola, H. Huttunen, and T. Virtanen, "Convolutional recurrent neural networks for polyphonic sound event detection," *IEEE/ACM Trans. Audio, Speech, and Language Processing*, vol. 25, no. 6, pp. 1291–1303, 2017.
- [15] Q. Kong, Y. Xu, W. Wang, and M. D. Plumbley, "Sound event detection of weakly labelled data with CNN-Transformer and automatic threshold optimization," *IEEE/ACM Trans. Audio, Speech, and Language Processing*, vol. 28, pp. 2450–2460, 2020.
- [16] K. Miyazaki, T. Komatsu, T. Hayashi, S. Watanabe, T. Toda, and K. Takeda, "Weakly-supervised sound event detection with self-attention," in *Proc. IEEE International Conference on Acoustics, Speech and Signal Processing (ICASSP)*, 2020, pp. 66–70.
- [17] —, "Conformer-based sound event detection with semi-supervised learning and data augmentation," in *Tech. Rep. DCASE Challenge*, 2020, pp. 1–5.
- [18] H. Saruwatari, T. Kawamura, T. Nishikawa, A. Lee, and K. Shikano, "Blind source separation based on a fast-convergence algorithm combining ICA and beamforming," *IEEE/ACM Trans. Audio, Speech, and Language Processing*, vol. 14, no. 2, pp. 666–678, 2006.
- [19] P. Smaragdis and G. J. Mysore, "Separation by "humming": User-guided sound extraction from monophonic mixtures," in *Proc. IEEE Workshop on Applications of Signal Processing to Audio and Acoustics (WASPAA)*, 2009, pp. 69–72.
- [20] T. Ochiai, M. Delcroix, Y. Koizumi, H. Ito, K. Kinoshita, and S. Araki, "Listen to what you want: Neural network-based universal sound selector," in *Proc. INTERSPEECH*, 2020, pp. 1441–1445.
- [21] Y. Okamoto, S. Horiguchi, M. Yamamoto, K. Imoto, and Y. Kawaguchi, "Environmental sound extraction using onomatopoeic words," in *arXiv, arXiv:2112.00209*, 2021, pp. 1–5.
- [22] O. Slizovskaia, G. Wichern, Z. Wang, and J. L. Roux, "Locate this, not that: Class-conditioned sound event doa estimation," in *arXiv, arXiv:2203.04197*, 2022, pp. 1–5.
- [23] D. Yang, H. Wang, Y. Zou, and C. Weng, "Detect what you want: Target sound detection," in *arXiv, arXiv:2112.10153*, 2021, pp. 1–5.
- [24] A. Dosovitskiy and J. Djolonga, "You only train once: Loss-conditional training of deep net works," in *Proc. International Conference on Learning Representations (ICLR)*, 2020, pp. 1–17.
- [25] E. Perez, F. Strub, H. Vries, V. Dumoulin, and A. Courville, "FiLM: Visual reasoning with a general conditioning layer," in *Proc. the Association for the Advancement of Artificial Intelligence (AAAI)*, 2018, pp. 1–17.
- [26] K. Imoto, S. Mishima, Y. Arai, and R. Kondo, "Impact of sound duration and inactive frames on sound event detection performance," in *Proc. IEEE International Conference on Acoustics, Speech and Signal Processing (ICASSP)*, 2021, pp. 860–864.
- [27] D. P. Kingma and J. Ba, "Adam: A method for stochastic optimization," in *Proc. International Conference on Learning Representations (ICLR)*, 2015.
- [28] J. Salamon, D. MacConnell, M. Cartwright, P. Li, and J. P. Bello, "Scaper: A library for soundscape synthesis and augmentation," in *Proc. IEEE Workshop on Applications of Signal Processing to Audio and Acoustics (WASPAA)*, 2017, pp. 344–348.
- [29] R. Serizel, N. Turpault, H. Eghbal-Zadeh, and A. P. Shah, "Large-scale weakly labeled semi-supervised sound event detection in domestic environments," in *Proc. Workshop on Detection and Classification of Acoustic Scenes and Events (DCASE)*, 2018, pp. 19–23.
- [30] Bilen Ç., G. Ferroni, F. Tuveri, J. Azcarreta, and S. Krstulović, "A framework for the robust evaluation of sound event detection," in *Proc. IEEE International Conference on Acoustics, Speech and Signal Processing (ICASSP)*, 2020, pp. 61–65.
- [31] X. Zheng, Y. Song, I. McLoughlin, L. Liu, and L. Dai, "An improved mean teacher based method for large scale weakly labeled semi-supervised sound event detection," in *Proc. IEEE International Conference on Acoustics, Speech and Signal Processing (ICASSP)*, 2021, pp. 356–360.
- [32] X. Zheng, H. Chen, and Y. Song, "Zheng USTC team's submission for DCASE2021 task4 - semi-supervised sound event detection," in *Tech. Rep. DCASE Challenge*, 2021, pp. 1–3.
- [33] J. Salamon, C. Jacoby, and J. P. Bello, "A dataset and taxonomy for urban sound research," in *Proc. 22nd ACM International Conference on Multimedia (ACM-MM'14)*, 2014, pp. 1041–1044.
- [34] X. Dong, B. Yin, Y. Cong, Z. Du, and X. Huang, "Environment sound event classification with a two-stream convolutional neural network," *IEEE Access*, vol. 8, pp. 125 714–125 721, 2020.

- [35] A. Mesaros, T. Heittola, and T. Virtanen, "Metrics for polyphonic sound event detection," *Applied Sciences*, vol. 6, no. 6, pp. 1–17, 2016.